

INFLUENCE OF NANO-TiO₂ CO-DEPOSITION ON THE MORPHOLOGY, MICROTOPOGRAPHY AND CRYSTALLINITY OF Ni/NANO-TiO₂ ELECTROSYNTHESIZED NANOCOMPOSITE COATINGS

A. I. PAVLOV^a, L. BENE^{a*}, J.-P. CELIS^b, L. VAZQUEZ^c

^a*Competences (Research) Centre Interfaces – Tribocorrosion and Electrochemical Systems, Faculty of Materials Engineering and Environment, Dunarea de Jos University of Galati, 47 Domneasca Street, 800008 Galati, Romania*

^b*Department of Metallurgy and Materials Engineering, MTM, Katholieke Universiteit Leuven, B-3001 Leuven, Belgium*

^c*Departamento de Superficies, Instituto de Ciencia de Materiales de Madrid (ICMM-CSIC), Sor Juana Inés de la Cruz 3, Cantoblanco, 28049 Madrid, Spain*

Ni-TiO₂ nanocomposites coatings with a layer thickness of 21 μm have been obtained by electrocodeposition. Incorporation in nickel matrix of TiO₂ nanoparticles (10 nm), affects the morphology of the nickel matrix as indicated from scanning electron microscope (SEM) and atomic force microscope (AFM) results. The chemical composition was studied by energy dispersive X-ray spectroscopy (EDS). Analysis by X-ray diffraction (XRD) revealed the inclusion of nickel particles in the matrix and their effect on nickel matrix crystal size changes.

(Received June 23, 2013; Accepted July 30, 2013)

Keywords: Electrochemical deposition, Nanocomposite coatings, SEM-EDS, AFM.

1. Introduction

Nanocomposites consisting of nano-particles included in a metallic matrix have attracted the attention of science and technology [1] which requires metallic materials with better surface properties [2]. Various techniques for developing composites were investigated and can be divided into two main groups: gas phase deposition methods - physical methods (PVD) and chemical methods (CVD); liquid phase deposition methods - chemical and electrochemical methods [1, 3, 4]. Among them, the electro-deposition method consisting in the incorporation of particles during electrolytic deposition has the advantages of rapidity, low cost, industrial applicability, ability to produce layers with sizes ranging from nm to μm [5] and homogenous distribution of the particles in the metallic matrix [6].

Another reason for choosing this technique is that the nanocomposite coatings may offer different properties such as wear resistance [7-11], corrosion protection [7-10], high resistance to oxidation [10] and hardness [11].

In the literature, the electrodeposition of metallic matrix with second phase particles such as TiO₂, Al₂O₃, CeO₂, SiC, TiC, ZrO₂, WC, ZnSe [1-2, 7-10, 12-17] have been reported. TiO₂ has three phases: anatase, rutile and brookite [3, 18]. Anatase TiO₂ is considered the most commonly phases [3] and one of the best photocatalysts [18]. The Ni-TiO₂ system was selected because nickel is an industrially important coating for corrosion protection [4] on support materials.

Compared with published data our experimental results present novelty in using 10 nanometer size of titanium oxide as dispersed phase during nickel electrocrystallization to obtain

*Corresponding author: lidia.benea@ugal.ro

Ni/nano-TiO₂ nanocomposite coatings on stainless steel support. The aim of this research was to synthesise nanocomposite coating having a nickel matrix by electro-co-deposition of nanometric TiO₂ dispersed phase (10 nm mean diameter) with nickel and to investigate the effects of such nanoparticles on the SEM-EDS surface and cross-section morphology and chemical composition, surface microtopography and X-Ray crystallinity of coatings obtained.

2. Experimental set-up

2.1 Materials and methods

Pure Ni coating noted with Ni/nano-TiO₂ (0 gL⁻¹) and nanocomposite coating noted with Ni/nano-TiO₂ (20 gL⁻¹) were prepared in a volume of 450 mL solution under conditions described in Table 1. A three electrode system was used to perform the experiments by positioning of the electrodes to parallel distance. Pure nickel plate was used as the anode; 304 stainless steel sheets with dimensions of 80 mm×50 mm×2 mm and area of 25 cm² was used as the cathode and a saturated calomel electrode (SCE) was used as the reference electrode.

Table 1 Chemical compositions and working parameters of the electrodeposition bath

Electrolyte composition	Amount
NiSO ₄ • 7H ₂ O	200 g/L
NiCl ₂ • 6H ₂ O	50 g/L
H ₃ BO ₃	30 g/L
TiO ₂	20 g/L
pH of solution	4.04
Temperature of the electrolyte bath	45 ± 1 °C
Current density	40 mA/cm ²
Deposition time	30 min
Magnetic stirring during electrodeposition	450 rpm

The titanium oxide nanopowder with particle size of 10 nm, used in this work was obtained from Hefei Kaier Nanometer Technology & Development Co. company and crystalline structure of this nanopowder is anatase with >99.99 % purity. During the electrodeposition process, the electrolyte was magnetically stirred at a rate of 450 rpm to be transported to the double layer at the cathode-electrolyte interface. In order to investigate the effect of nanoparticles in the electrodeposition process, the coatings was deposited on 304 stainless steel after electroplating for 30 min at a current density of 40 mA/cm². For comparison, pure Ni coatings were also prepared in the same solution mentioned above except TiO₂ nanoparticles, which were not introduced, under the same electrodeposition conditions. The thickness of the produced coatings was at least 21 μm and was verified by measuring the weight before and after deposition.

The codeposition experiments were conducted by using a potentiostat/galvanostat model PGZ 100.

2.2 Characterization of nanocomposite coatings

Surface morphologies of coatings and cross-section of layer thickness were examined by scanning electronic microscope (SEM) using Philips model XL 30 FEG. The chemical composition of coatings and the concentration of TiO₂ nanoparticles into Ni-TiO₂ nanocomposite coatings were evaluated by energy dispersive X-ray spectroscopy (EDS) system attached to the SEM.

The cross-sections of the samples were prepared by cutting and embedding them in a resin to be after mechanical polished with silicon carbide paper and diamond suspension down to 1 μm . Then the samples were cleaned with distilled water and ethanol. Before SEM-EDS examinations the samples were coated with a thin layer of gold (Au) for 40 sec. Atomic force microscopy (AFM) was used for studying the surface topography and roughness of the coating surfaces using Agilent Picoplus 5500 device. The measurements were made in the dynamic mode (also called tapping mode).

X-ray diffraction analysis was carried out using a Seifert 3003 T diffractometer, with a Cu-K α radiation. Diffractograms were recorded with a voltage of 40 kV, current of 40 mA, step size of 0.02° for 2 θ ranging from 10 to 100° and measuring time 2s per step. The phases present in the coatings can be identified with a special X-Ray identifying program.

3. Results and discussions

Analysis of electroplated layers by electron microscopy, revealed differences in surface morphology of nanocomposite compared to pure nickel electrodeposition. Figure 1 (a) shows SEM surface morphology image and EDS spectrum analysis for pure nickel samples, called Ni/nano-TiO₂ (0 gL⁻¹). The same conditions for electrodeposition (current density and time) were used to obtain Ni/nano-TiO₂ (20 gL⁻¹) nanocomposite coatings and the SEM-EDS analysis is presented in Figure 1 (b).

As we can see from Figure 1 the two types of surfaces have different morphological forms. Analysis was done on full sample surface under 3000 \times magnification with accelerating voltage of 10 kV.

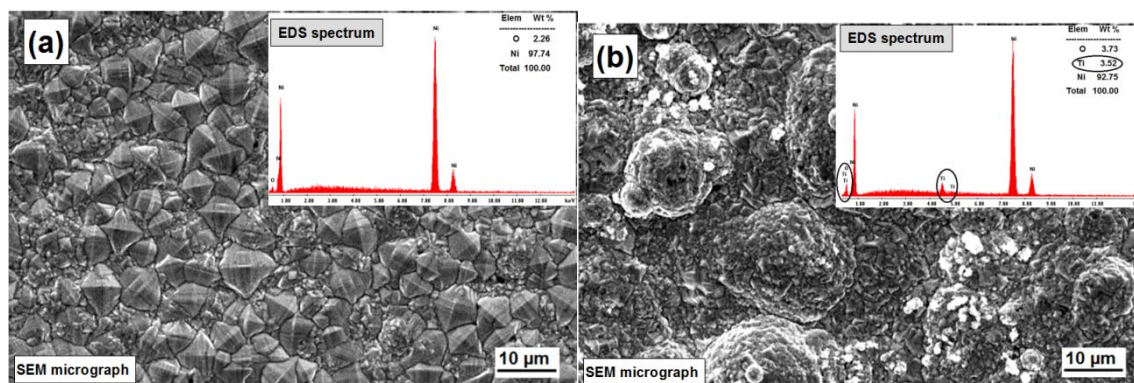


Fig. 1 SEM surface micrographs and EDS spectrum analysis of:
(a) Ni/nano-TiO₂ (0 gL⁻¹) coating and (b) Ni/nano-TiO₂ (20 gL⁻¹) nanocomposite coating

By adding the TiO₂ nanoparticles into nickel matrix by electro-co-deposition, the morphology of nickel matrix is changed and the nickel crystal size of deposits becomes smaller as it is illustrated in Figure 1 (b) where as light spots as validated by energy dispersive X-ray spectroscopy appears. Similar results were reported by other authors [19]. The pseudo-pentagonal crystal symmetry is typical for a pure nickel deposit according to others authors [20] as it is shown in Figure 1 (a). This crystal symmetry and morphology of pure nickel is much changed by adding TiO₂ nanoparticles to obtain nanocomposite coating, as it is observed in Figure 1 (b). From EDS spectrum (Figure 1), it is observed that for pure nickel coatings there is a small signal for oxygen coming from the in-staneous oxide film formed, meanwhile the EDS spectrum for nanocomposite coating shows the presence of TiO₂ nanoparticles into the coating by titanium signal and a higher content of oxygen. The mean titanium content was obtained at wt. 3.52% resulting a TiO₂ content into composite coating at about 6.6 wt.% (appreciated from surface analysis).

Figures 2 and 3 show the cross-section of pure nickel and nanocomposite coatings. From these figures we could observe that the thicknesses of pure Ni coating and the Ni/nano-TiO₂ (20 gL⁻¹) nanocomposite coating have similar values of about 21 μm. The same figures show a good adhesion of pure nickel and nanocomposite coatings with the stainless steel substrate.

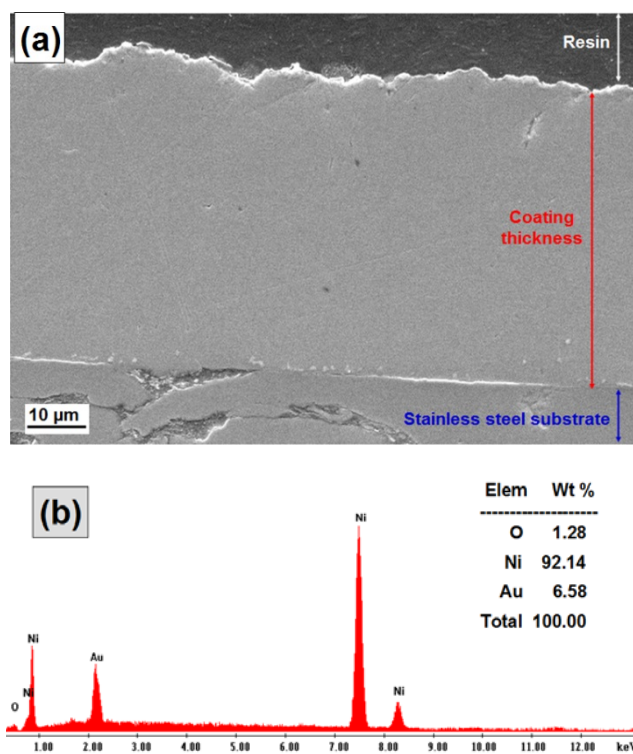


Fig. 2 SEM-EDS cross-section coating thicknesses analysis of:
(a) SEM image and (b) EDS spectrum for electrodeposited Ni/nano-TiO₂ (0 gL⁻¹) layer.

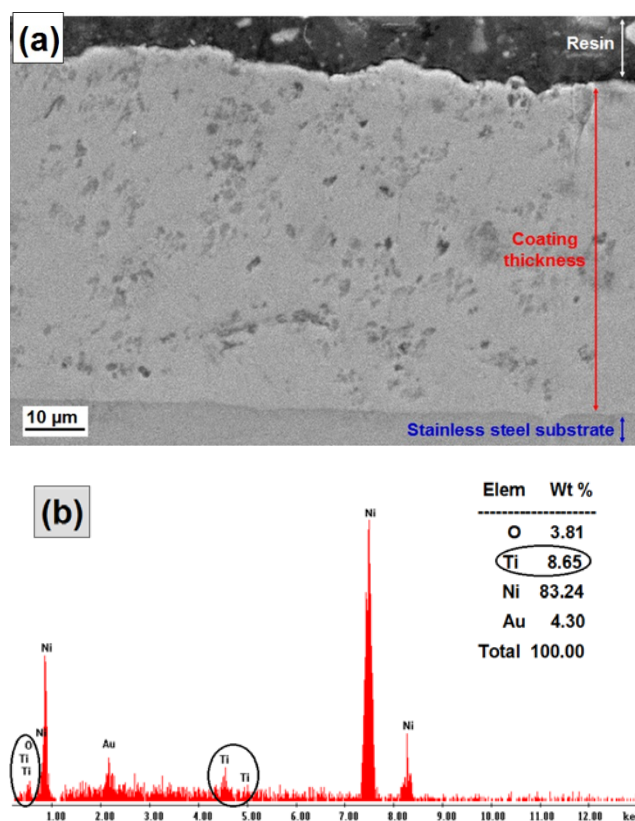


Fig. 3 SEM-EDS cross-section coating thicknesses analysis of: (a) SEM image and (b) EDS spectrum for electrodeposited Ni/nano-TiO₂ (20 gL⁻¹) nanocomposite coating.

From EDS analysis of nanocomposite coating presented in Figure 3 (b) it can be seen the presence of dispersed TiO₂ phase into nickel matrix. The content of Ti signal resulted at a value of wt. % 8.65 being higher than that obtained for the surface. Therefore the TiO₂ content into cross section of the nanocomposite coating was calculated at a higher value than that on the surface, respectively at wt. 16 %.

Figures 1(b) and Figure 3 show also that TiO₂ nanoparticles are uniformly dispersed into the nickel matrix on the surface as well as, through the cross-section of the nanocomposite coatings.

From AFM microtopographic 3D images (80 µm×80 µm area) presented in Figure 4 we could see the increasing of roughness (R_a) from 0.196 µm for Ni/nano-TiO₂ (0 gL⁻¹) to 0.536 µm for Ni/nano-TiO₂ (20 gL⁻¹). Both types of coatings were deposited at a current density of 40 mA/cm² confirming the disturbance effect of nanoparticles inclusion to surface morphology and topography of nickel matrix. The roughness (R_a) increases due to addition of TiO₂ nanoparticles both on the ridges and valleys of the nickel facets. Similar results were reported by other researchers [21].

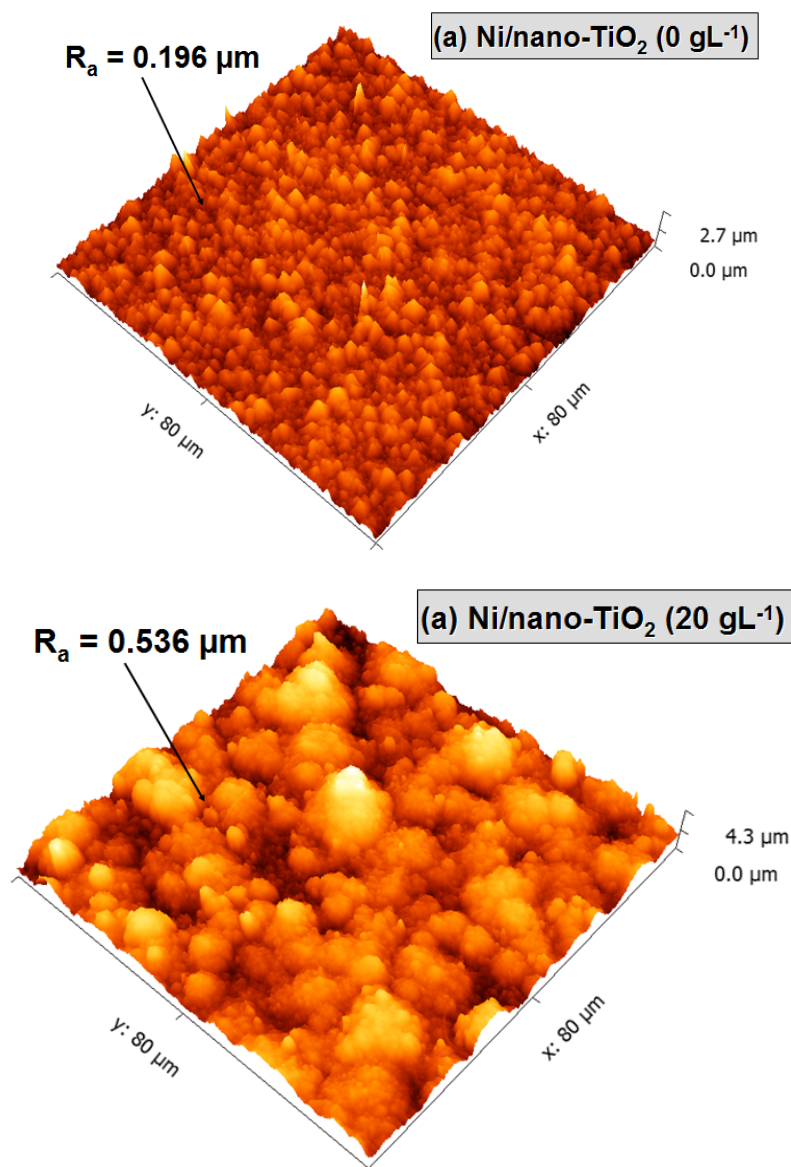


Fig. 4 AFM microtopographic 3D images of:
(a) Ni/nano-TiO₂ (0 gL⁻¹) layer and (b) Ni/nano-TiO₂ (20 gL⁻¹) nanocomposite coating.

Representative XRD patterns of coatings produced are presented in Figure 5. XRD study was carried out on the electrocoated samples to identify the phases and modification of representative diffraction peaks of nickel due to the inclusion of TiO₂ nanoparticles into nickel matrix during electrodeposition. The diffractograms are characterised by (1 1 1), (2 0 0), (2 2 0), (3 1 1) and (2 2 2) diffraction peaks.

From Figure 5 it can be seen that the coatings exhibited face-centered cubic (fcc) lattice. The XRD diagram of pure Ni deposit (Figure 5 a) is characterized by a strong (1 1 1) line at $2\theta = 44.34^\circ$, while for nanocomposite coating (Figure 5 b) we can notice about the same intensity for (1 1 1) peak, the decreasing of (2 0 0) and (3 1 1) peaks, and an increasing of (2 2 0) peak. The (2 2 2) peak is kept at the same intensity for both types of coatings. Similar X-ray diffraction patterns of the electrodeposited nanocrystalline nickel coatings were obtained by other researchers [1, 6, 19, 21] during electroplating of pure nickel coating.

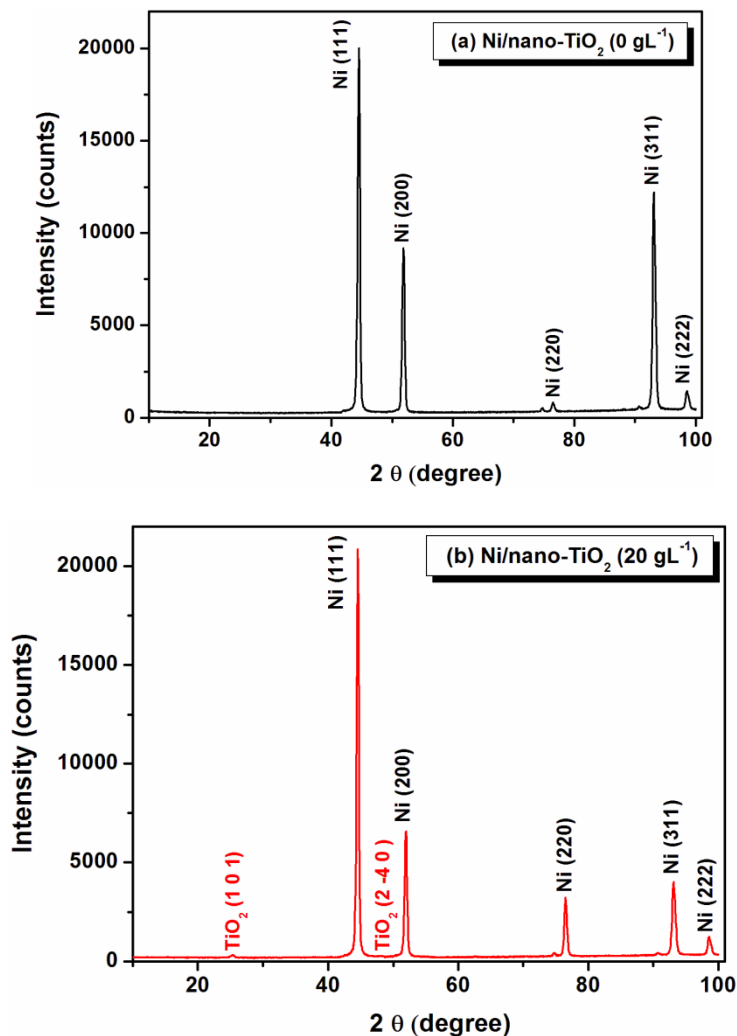


Fig. 5 X-ray diffraction patterns of:
 (a) Ni/nano-TiO₂ (0 gL⁻¹) and (b) Ni/nano-TiO₂ (20 gL⁻¹) coatings obtained by electrodeposition.

Other researchers as D. Thiemi^g et al. [1], S.A. Lajevardi et al. [19], S. Spanou et al. [20] have reported in their work as the reflection at $2\theta = 25.3^\circ$ can be assigned to the (1 0 0) orientation of anatase. Our XRD analysis has identified a new line (1 0 1) at approximately the same reflection of $2\theta = 25.34^\circ$ as anatase with reference code 01-086-1155 from identification program of phases. The peak from $2\theta = 43.67^\circ$ can be assigned to the (2 -4 0) line and confirms the presence of TiO₂ as dispersed phase into nanocomposite coating, as it can be seen in Figure 5 (b).

4. Conclusions

The experiments from this paper have shown new insights in obtaining the nanocomposite coating with dispersed TiO₂ nanoparticles by electro-co-deposition method. Our investigation indicated that by embedding the TiO₂ nanoparticles into Ni matrix the surface morphologies of the resulted nanocomposite coatings are affected.

The analyses of the samples in cross-sectional preparation give information about the layer thicknesses as well as about the presence of the second TiO₂ dispersed phase into nickel matrix.

From AFM microtopographic 3D images it was observed the increasing of roughness of nanocomposite coating as compared with pure Ni coating, confirming the disturbance effect of nanoparticles inclusion to surface morphology and topography of nickel matrix.

From XRD patterns of coatings it was observed the inclusion of nanoparticles into metallic matrix and their effects on crystallinity and structure of nickel matrix. The preferred orientation of pure nickel coating is disturbed by TiO₂ nanoparticles inclusion to a nonpreferred one.

We are further optimising the processing and properties of this nanocoatings technology in an effort to use it in industrial applications.

Acknowledgements

The preparation of this paper would not have been possible without the support provided by the Bilateral Research Agreement between Research (Competences) Centre Interfaces – Tribocorrosion and Electrochemical Systems (CC-ITES) from Dunarea de Jos University of Galati and Department of Metallurgy and Materials Engineering (MTM) from Katholieke Universiteit Leuven. This work was financially supported by the research Project IFA-CEA C2-02/01/03/2012.

References

- [1] D. Thiemi, A. Bund, *Surf. Coat. Technol.* **202**, 2976-2984 (2008).
- [2] P. Wang, Y.-l. Cheng, Z. Zhang, *J. Coat. Technol. Res.* **8**, 409-417 (2011).
- [3] X. Chen, *Chin. J. Catal.* **30**, 839-851 (2009).
- [4] O. Sadiku-Agboola, E. R. Sadiku, O. I. Ojo, O. L. Akanji, O. F. Biotidara, *Port. Electrochim. Acta* **29**, 91-100 (2011).
- [5] I. Gurrappa, L. Binder, *Sci. Technol. Adv. Mater.* **9**, 1-11 (2008).
- [6] P. Gyftou, E. A. Pavlatou, N. Spyrellis, *Appl. Surf. Sci.* **254**, 5910-5916 (2008).
- [7] C. S. Lin, C. Y. Lee, C. F. Chang, C. H. Chang, *Surf. Coat. Technol.* **200**, 3690-3697 (2006).
- [8] P. Bagheri, M. Farzam, A. B. Mousavi, M. Hosseini, *Surf. Coat. Technol.* **204**, 38040 (2010).
- [9] R. Sen, S. Das, K. Das, *Surf. Coat. Technol.* **205**, 3847-3855 (2011).
- [10] M. R. Vaezi, S. K. Sadrezaad, L. Nikzad, *Colloids and Surfaces A: Physicochem. Eng. Aspects* **315**, 176-182 (2008).
- [11] M. Lekka, C. Zanella, A. Klorikowska, P. L. Bonora, *Electrochim. Acta* **55**, 7876 (2010).
- [12] B. M. Praveen, T. V. Venkatesha, *Appl. Surf. Sci.* **254**, 2418-2424 (2008).
- [13] L. Benea, F. Wenger, P. Ponthiaux, J.P. Celis. *Wear.* 266, (3-4), 398-405 (2009).
- [14] M. Karbasi, N. Yazdian, A. Vahidian, *Surf. Coat. Technol.* **207**, 587-593 (2012).
- [15] L. Benea, *J. Appl. Electrochem.* **39**, 1671-1681 (2009).
- [16] L. Kodandarama, M. Krishna, H. N. Narasimha Murthy, S. C. Sharma, *JMEPEG* **21**, 105-113 (2012).
- [17] S. R. Kumar, M. Nuthalapati, J. Maity, *Scripta Mater.* **67**, 396-399 (2012).
- [18] D. Mardare, N. Cornei, G. I. Rusu, *Superlattices and Microstructures* **46**, 209-216 (2009).
- [19] S. A. Lajevardi, T. Shahrabi, *Appl. Surf. Sci.* **256**, 6775-6781 (2010).
- [20] S. Spanou, E. A. Pavlatou, N. Spyrellis, *Electrochim. Acta* **54**, 2547-2555 (2009).
- [21] G. Parida, D. Chaira, M. Chopkar, A. Basu, *Surf. Coat. Technol.* **205**, 4871-4879 (2011).